MODELLING OF A THREE-LAYER SEDIMENT TRANSPORT SYSTEM IN OSCILLATORY FLOW

Leszek M. Kaczmarek & Rafał Ostrowski[1]

Abstract

An extension of the bedload model of Kaczmarek & Ostrowski (1996), taking account of suspended sediment, is proposed for the calculation of sediment transport features, such as the transport rate and thickness. The paper is focused on the transition region (named as a contact load layer) between the outer region (suspension layer) and the bedload layer within the proposed three-layer sediment transport model.

Theoretical background

Formulation of the problem

A typical vertical distribution of velocity at a rough bed is supposed to be characterised by a sub-bottom flow and a main or outer flow, as shown in Fig. 1. The figure provides an explanatory drawing with velocities and concentrations. The collision-dominated granular-fluid region stretches below the nominal static bed while the wall-bounded turbulent fluid region extends above it. The outer region of pure suspension is characterised by very small concentration, where the process of sediment distribution may be considered as a convective and (or) diffusive process. In contrast, the granular-fluid region below the nominal bed is characterised by very high concentrations, where the intergranular resistance is predominant.

Since both water and grains are assumed to move in both regions, there must be a certain transition zone between these two regions, in which the velocity and stress profiles merge and preserve continuity of shape. The transition zone, called a contact load layer, is a central topic of the present study. The velocity profile in the contact load layer is assumed to be continuous. Its intersection with nominal seabed is the

[1] Snr. Research Associates, Polish Academy of Sciences' Institute of Hydro-Engineering *IBW PAN*, 7 Kościerska, 80-953 Gdańsk, Poland

apparent slip velocity u_b which can be identified as a characteristic velocity of sediment moving in the form of bedload. The downward extension of the velocity distribution in the outer zone of the main flow yields a fictitious slip velocity u_0 of the fluid at the nominal static bed level. Clearly, the fluid velocity u_0 is greater than the sediment velocity u_b.

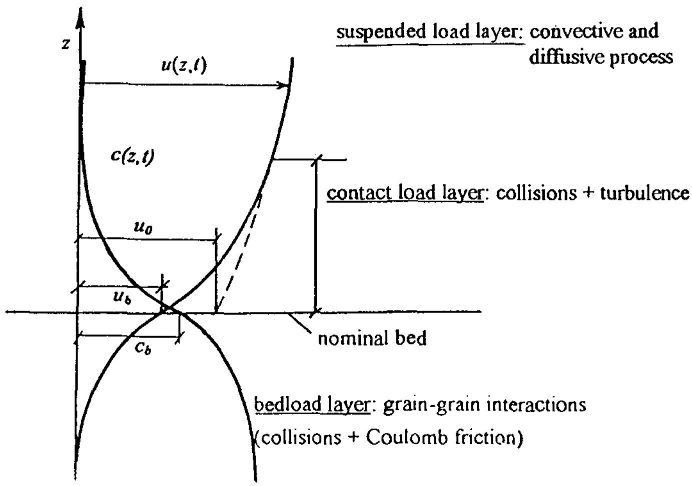

Fig. 1. Definition sketch

The above three-layer system of the momentum exchange has recently been observed in the measurements of concentrations carried out by Ribberink & Al-Salem (1995).

Physical bases

It is traditionally assumed, see for instance Wilson (1987), that the contact load layer consists of several layers of grains in motion, and in these layers the applied shear stress τ is resisted by the sum of a granular component τ_s and a fluid component τ_f. As demonstrated by Bagnold (1956), τ_s is associated with the intergranular stresses due to particle collisions. The sheared layer extends down to a certain level (say nominal bed) at which the intergranular resistance τ_s equals the applied shear stress τ. Further down towards the non-moving bed the intergranular resistance is predominant and it can be assumed that the particle interactions in the bedload layer produce two distinct types of behaviour. The particle collisions give rise to viscous-type stresses, while further down towards the non-moving bed, Coulomb friction between particles (which remain in contact with each other) give rise to plastic-type stresses.

Because the intergranular resistance is predominant in the bedload layer, it is postulated that the weight of moving sediment is transferred to the grain skeleton in the non-moving bed.

In contrast, the sediment in the contact load layer is transported partially as a bedload and partially as a suspended load. This means that the sediment is carried both by the dispersive stresses and by the fluid. When the suspended sediment is carried by the fluid, its weight causes an increase in the pressure above the hydrostatic. Hence, it can not be assumed that the stress transferred to the bedload layer from the contact load layer corresponds exactly to the weight of the load. This was illustrated by Deigaard (1993) who considered a grain jumping in fluid.

Grain-grain-water interactions in the contact load layer are assumed to produce three distinct types of behaviour. The random motion of the sediment grains, which is the basis for the diffusion process, is caused by a combination of turbulence and the collisions between the grains in the contact load layer. These two effects give rise to skin friction τ'. Aside from the skin friction, a particle exposed to a turbulent flow will additionally feel a drag due to a pressure difference on the up- and downstream sides of the grain because of flow separation. Thus, the residual part of the total shear stress $\tau-\tau'$ is carried as a drag on the moving bed particles. This drag gives rise to a convective sediment exchange rather than to turbulent diffusion.

The above shows that the two layers, e.g. bedload and contact load, differ considerably in momentum exchange. Hence, the interface between them, i.e. the level at which the intergranular resistance equals the applied total shear stress, can be expected as a very distinct one. This is supported by the recent measurements of concentration carried out by Ribberink & Al-Salem (1995). The detailed concentration measurements showed a three-layer system with a lower and upper sheet flow layer and a suspension layer. The lower and upper sheet flow layer can be identified as bedload and contact load layers, respectively. Sediment was picked up from the lower sheet flow layer at the two phases of maximum velocity during the wave cycle, resulting in two concentration dips in the lower sheet flow layer and two concentration peaks in the upper sheet flow layer.

Solution procedure

It is next proposed that the downward extension of the velocity distribution from the suspension layer to the bedload layer is described by the logarithmic distribution and is controlled by effective bed roughness k_e. The logarithmic velocity profile extrapolated from the suspension region is positioned at $z_0=k_e/30$, the height where the velocity profile approaches zero. Further, the flow at the top of the contact load layer is assumed to be unaffected by the transition phenomena.

These assumptions allow to solve the problem of nearbed sediment motion within two steps, schematically shown in Fig. 2. Within the first step, the problem is reduced to bedload transport (Fig. 2a) the solution of which was proposed in a series of papers by Kaczmarek et al. (1994), Kaczmarek et al. (1995) and Kaczmarek & Ostrowski (1996), who used a theoretical approach based on grain-grain interaction ideas in analogy to the flow of dry, cohesionless materials. The iterative procedure was employed to match the velocity and shear stress profiles in both regions (Fig. 2a) using a theoretical bed level for the outer wave-induced flow of δ_{sx}, which was taken as an arbitrary fraction of the thickness of the moving, collision-dominated bed layer δ_n.

The motion of sediment inside the contact load layer is proposed to be solved within the second step (Fig. 2b). In this case the problem is focused on finding of skin effective roughness k_e' with determination of the thickness δ_c of the contact load layer. As a boundary condition it is proposed to use the instantaneous (during wave period) sediment velocity $u_b(t)$ and concentration c_b (assumed to be constant and equal to 0.32) at the top of bedload layer, found from the bedload model with δ_{sx}/δ_n=0.50.

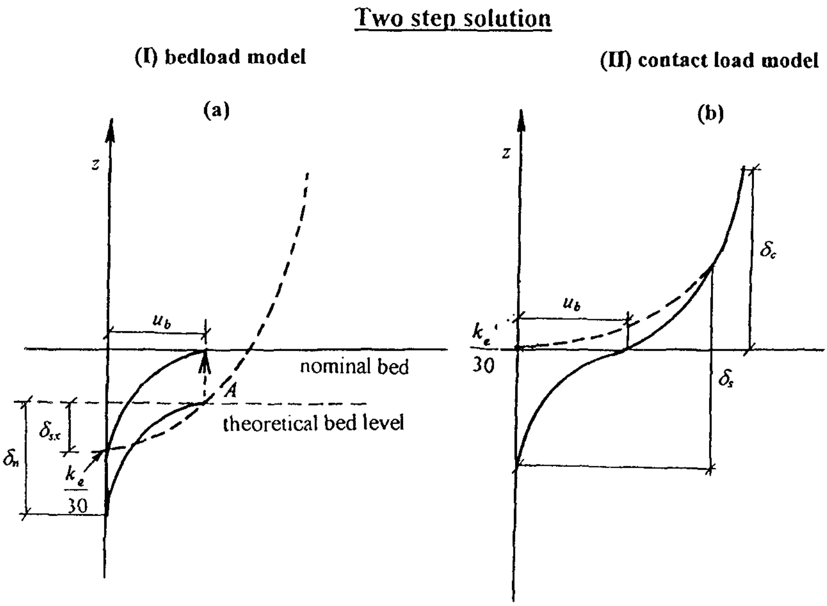

iteration procedure for finding matching point A with determination of δ_{sx} and k_e

finding skin effective roughness k_e' with determination of δ_c using u_b as boundary condition, found from step (I)

Fig. 2. Solution procedure

Basic equations and solution

Bedload layer

The bedload sediment transport model is based on a collision-dominant drag concept and uses a single parameter, δ_{sx}, to define the theoretical level of the top of the moving bedload layer in relation to the effective roughness height, k_e, of the above-bed wave-induced flow.

Previous comparison of model results with experimental data for sediment transport rates and thicknesses, presented by Kaczmarek et al. (1995) and Kaczmarek & Ostrowski (1996), had suggested a value of δ_{sx}/δ_n=0.5. The use of the single constant parameter δ_{sx}/δ_n=0.5 yields the effective roughness height decreasing with the increase of the grain roughness Shields parameter $\theta_{2.5}$, the definition of which is given by Nielsen (1992). This decreasing trend is related to the constant value of δ_{sx}/δ_n ratio kept for the entire range of $\theta_{2.5}$, see Fig. 3.

It is possible, however, to determine the variation of δ_{sx}/δ_n with $\theta_{2.5}$ (see Fig. 4) so that the model reproduces the variation in apparent roughness k_a observed by Nielsen (1992) for (artificially) flat beds, see Fig. 3.

Next, using the variable δ_{sx}/δ_n values, calculations were made to find bedload properties such as bedload thickness and transport rate. These calculations have been carried out for a wide range of wave heights and for two sets of depth and period values, i.e. h=5 m, T=3.6 s and h=10 m, T=8.39 s, with grain diameter d=0.2 mm for both sets of parameters and additionally d=0.7 mm for the long-period data set. The results of computations shown in Fig. 5 reveal that the present approach with the fitting parameter k_e given by Nielsen (1992) provides a good approximation of bedload thickness $L_{B,max}$ for (artificially) flat beds at low flow intensities ($\theta_{2.5}\leq 0.4$). In the range of relative effective roughness values with $\theta_{2.5}$>0.4 the theoretical results overestimate the experimental data. It seems that, for this range of $\theta_{2.5}$, the present approach with the fitting parameter k_e resulting from constant ratio δ_{sx}/δ_n=0.5, provides a better estimation of bedload thickness. The same conclusions can be drawn from the calculations of bedload rate carried out for both fixed and variable values of δ_{sx}/δ_n.

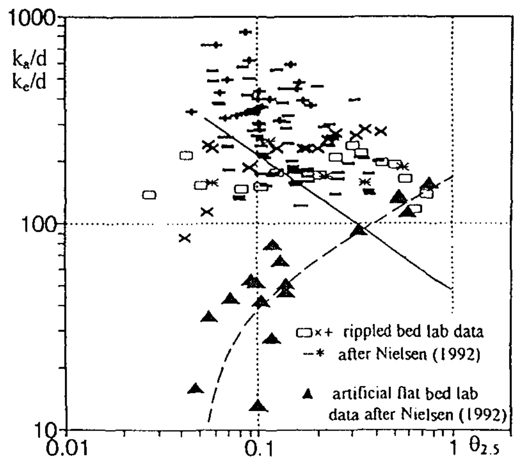

Fig. 3. Comparison of an apparent roughness found from friction and dissipation lab. data (k_a) with computed effective roughness (k_e) for δ_{sx}/δ_n=0.5 (solid line) and for variable δ_{sx}/δ_n (dashed line)

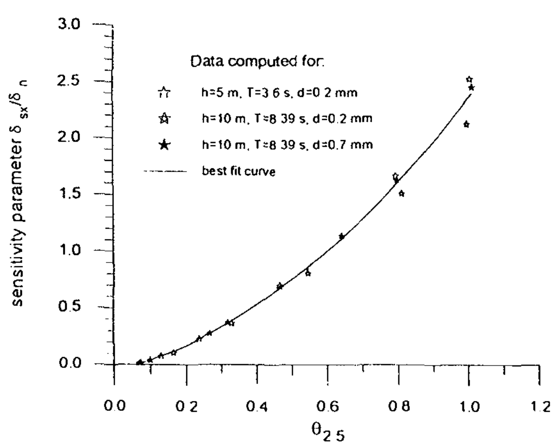

Fig. 4. Variation of sensitivity parameter δ_{sx}/δ_n with $\theta_{2.5}$

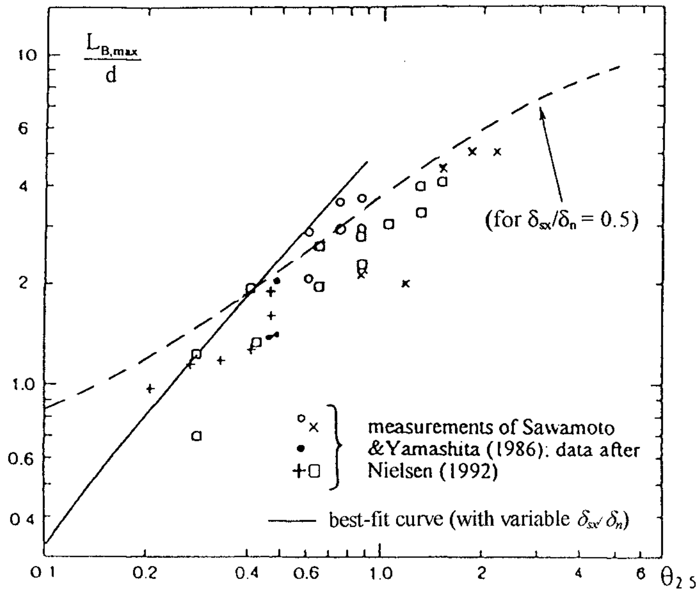

Fig. 5. Model bedload thickness $L_{B,\max}$ (with variable δ_{sx}/δ_n) vs. lab. measurements of Sawamoto & Yamashita, data and definition of $L_{B,\max}$ after Nielsen (1992)

Contact load layer

Following Fernández Luque's, after Fredsøe & Deigaard (1992), and Engelund & Fredsøe's (1976) ideas, the momentum transfer in the contact load layer can be described by the equation:

$$\tau = \overbrace{\tau_f + \tau_s}^{\tau'} + nF_D \tag{1}$$

where F_D is the average drag on a single moving particle, while n is the number of moving particles per unit area.

It is assumed that the moving particles in the contact load layer reduce the fluid shear stress τ_f by exerting an average reaction force on the surrounding fluid. This reduction, however, is not so drastic as it is inside the bedload layer, where the intergranular resistance is predominant. Further, it is proposed that the velocity gradient inside the contact load layer is affected by the presence of sediment.

A new formulation for skin friction, which is considered as a combination of turbulence and the collisions between the grains, is proposed. A new model of sheet flow is developed, incorporating the diffusion concept presented by Deigaard (1993).

By assuming that the settling of sediment balances the vertical exchange, and that the momentum exchange balances the shear stress, Deigaard (1993) proposed two coupled differential equations to determine the mean concentration profile and the velocity profile:

$$\left[\frac{3}{2}\left(\alpha\frac{d}{w_s}\frac{du}{dz}\frac{2}{3}\frac{s+c_m}{c_d}+\beta\right)^2 d^2c^2(s+c_m)+l^2\right]\left(\frac{du}{dz}\right)^2=u_f'^{\,2} \tag{2}$$

$$\left[3\left(\alpha\frac{d}{w_s}\frac{du}{dz}\frac{2}{3}\frac{s+c_m}{c_d}+\beta\right)^2 d^2\frac{du}{dz}c+l^2\frac{du}{dz}\right]\frac{dc}{dz}=-w_sc \tag{3}$$

in which w_s denotes settling velocity of grains, s is a relative sediment density, c_m and c_d are the added mass and drag coefficients, respectively, and l is a mixing length defined as $l=\kappa z$.

In general, two coefficients α and β have to be determined, e.g. by calibration. For simplicity, equal values of α and β have been assumed in further considerations. The boundary conditions for these equations are that the sediment velocity u and concentration c are given at the top of bedload layer positioned in the model at $k_e'/30$. In the calculations the sediment concentration at $z=k_e'/30$ was assumed as 0.32 (in agreement with the bedload model). It was further assumed that $(s+c_m)=3.0$ and $c_d=1.0$.

It is still unclear how to evaluate the drag due to moving sand particles. It is possible, however, to overcome these difficulties making an additional assumption that the sediment velocity distribution in the contact load layer is controlled by the effective skin roughness k_e' and that the sediment velocity profile attains a logarithmic shape at a certain distance from the nominal bed. Making use of the above, sediment motion in the contact load layer is determined by Eqs. (2) and (3) and by the following relationship:

$$\tau'=\tau-nF_D=\rho u_f'^{\,2} \tag{4}$$

in which u_f' is the skin friction velocity, proposed to be found using Fredsøe's (1984) integral momentum model with k_e' specified as a fixed constant value. Following Nielsen (1992) a value of $2.5d$ was adopted for the effective skin roughness k_e' of the moveable flat bed.

Knowing the instantaneous (during the wave period) skin shear stress $\rho u_f'^2(t)$ it is possible to calculate sediment concentration $c(z,t)$ and velocity $u(z,t)$ in the contact load layer using Eqs. (2) and (3) with the boundary conditions u_b (t) and c_b given at $z=k_e'/30$ from the bedload solution with $\delta_{sx}/\delta_n=0.50$. The proposed solution depends on the coefficient α $(=\beta)$. Making use of the fact that the velocity attains a logarithmic shape at a certain distance from the bed and that the roughness corresponding to this logarithmic profile depends on α, an iterative procedure is postulated to find α $(=\beta)$. The sought value of α $(=\beta)$ must provide the match of velocity profile yielded by Eqs. (2) and (3) with the logarithmic profile described by the skin friction parameters (k_e' and u_f'). The match is found at the moment corresponding to the maximum skin shear stress.

The model solution is restricted by a number of simplifying assumptions. Therefore, the determination of the layer thickness δ_c identified as the solution validity limit plays a very important role. The selection criterion for δ_c can be based on the degree of fit to experimental data comprising sediment concentrations and transport rate within the contact load layer. In the next section, two values for the upper limit of the contact load layer are tested against laboratory data, namely $\delta_l/4$ and $\delta_l/2$, where δ_l is the thickness of the bed boundary layer $\delta(t)$ calculated from Fredsøe's (1984) model at the moment corresponding to maximum free stream velocity. The quantity $\delta_1/2$ can be identified as the conventional bottom boundary layer thickness while $\delta_1/4$ denotes upper limit of the region where the logarithmic velocity profile is observed.

Finally, it is worthwhile noting that the turbulence damping by the suspended particles is represented in the model by the following relationships:

$$\varepsilon_s = \beta_1 \cdot \varepsilon = \beta_1 \cdot \kappa \cdot u_f \cdot z \tag{5}$$

$$\varepsilon_s = \kappa \cdot z \cdot (\beta \cdot u_f) = \kappa \cdot z \cdot u_f{}' \tag{6}$$

in which ε_s is the mixing coefficient for solid material, κ is von Karman's constant (=0.4) and β_1 is a factor which, according to Deigaard, after Fredsøe & Deigaard (1992), is always smaller than the turbulent momentum exchange coefficient ε, with difference proportional to w_s/u_f.

Comparison with experimental data

Reference concentration and sheet flow layer thickness

The model has been run for two sets of water depth and wave period (h=10 m, T=8.39 s and h=5 *m*, T=3.6 s) and for the grain diameter d=0.2 mm. In addition, the first set of depth and period values has been run for the grain diameter d=0.7 mm. The wave height has been changed in each run so that a wide range of sediment transport intensities has been analysed. The model results for concentration at z=1.5d has been compared with the experimental data of Guy et al., as interpreted by Zyserman & Fredsøe (1994). The comparison, shown in Fig. 6, yields quite good agreement.

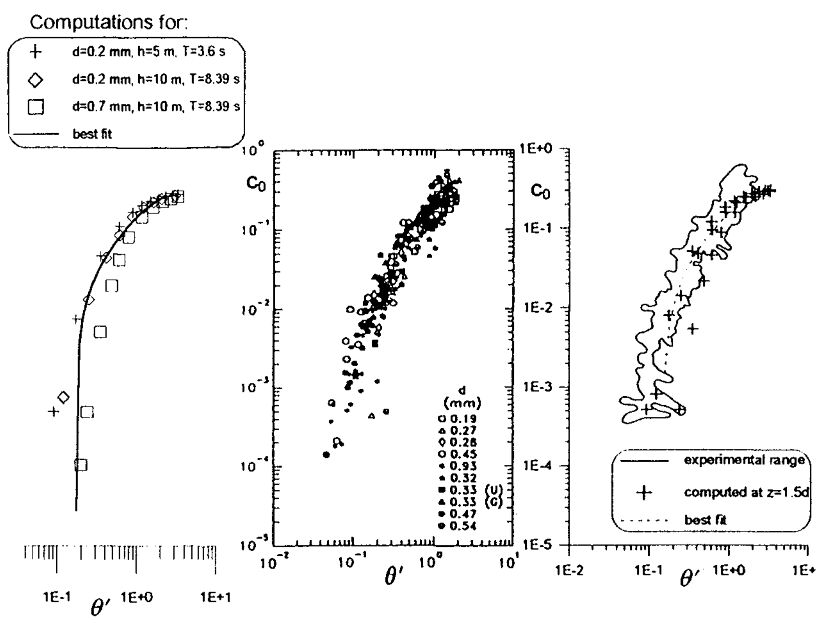

Fig. 6. Reference concentration c_0: model results vs. experimental data of Guy et al. as interpreted by Zyserman & Fredsøe (1994)

The same sets of computational parameters have been used in the modelling of the sheet flow layer thickness δ_s. The upper limit of this layer has been interpreted as the level at which the model result for velocity at the moment corresponding to the maximum skin shear stress attains the logarithmic velocity distribution with the accuracy of 99%. The distance between the above defined level and $z=k_e'/30$, summed up with the bedload layer thickness, yields the sheet flow layer thickness and is shown in Fig. 7 as a function of dimensionless maximum skin shear stress, i.e. $\theta'=u_f'^2/[(s-1)gd]$. It can be seen that the sheet flow layer thickness, even in very severe storm conditions, does not exceed 20 grain diameters. Good agreement between theoretical findings for the sheet flow layer thickness from the present model and the experimental data of Sumer et al. (1996) has also been found, see Fig. 7.

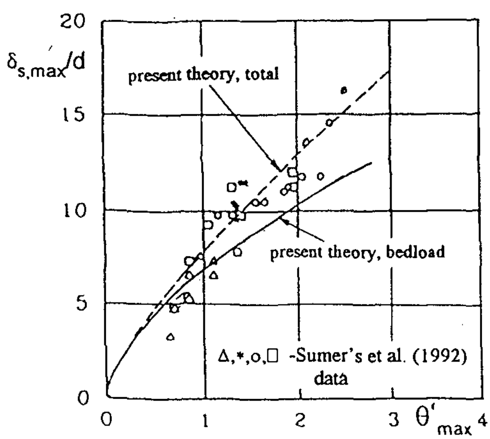

Fig. 7. Sheet flow layer thickness: model results vs. experimental data of Sumer et al. (1996)

Time-dependent and mean concentration

The data used in the present comparisons were obtained by Ribberink & Al-Salem (1994, 1995) for regular symmetric and asymmetric waves. The experiments were carried out in the Large Oscillating Water Tunnel (LOFT) at Delft Hydraulics. All the data were obtained above plane sand beds, corresponding to very vigorous conditions in nature, with median grain diameter $d=d_{50}=0.21$ mm. Suspended sediment concentrations were measured principally with an optical concentration meter (OPCON) while concentrations in the sheet flow layer were measured using a conductivity concentration meter (CCM), see Al-Salem (1993) for details.

In the comparisons discussed below the aim has been to compare the model predictions with emphasis on time-variation in sediment concentration $c(z,t)$ at different heights (z) above the bed. The data sets used for this purpose are the series „C" experiments: Conditions 1 and 2 for asymmetric waves, with $U_{rms}=0.6$ m/s, $T=6.5$ s and $U_{rms}=0.6$ m/s and $T=9.1$ s, respectively, and Condition 3 for sinusoidal wave, with $U_{rms}=1.2$ m/s and $T=7.2$ s.

In Fig. 8 the exemplary model predictions for Condition 2 are compared with time-varying sediment concentrations $c(z,t)$ measured at two representative ordinates with respect to the original bed level z=0 (i.e. the undisturbed bed level prior to the start of the experiment, identified as $z=k_e'/30$ in the model). The curve for z=-1 mm has been produced (for the time sectors in which the sediment movement occurs) using the bedload model while for z=+1 mm the concentration has been computed by the present contact load model. At both levels the prediction shows satisfactory agreement with the data. The concentration at z=0 is assumed as c_b=0.32=848 g/l (with grain density of 2650 kg/m^3).

At higher levels, however, the measured time series of $c(z,t)$ develops a more complicated structure, and agreement in phase between the model and the data is lost. The reason for the failure of the model to predict the phase angle of the time-dependent concentration is the appearance, at around the time of flow reversal in the free stream between wave crest and trough, of an additional peak in sediment concentration, identified by Davies et al. (1997) as a convection peak. Near the bed (roughly up to $z=\delta_1/4$) this peak is very small and the time series of concentration is dominated by the main diffusion peak associated with the maximum velocity, and hence maximum bed shear stress, during the wave cycle. With increasing height, the additional peak grows in relative importance, becoming larger than the diffusion peak and dominating the concentration time series.

Hence, the ordinate of $\delta_1/4$ (which corresponds to z=0.5 cm for Condition 2) determines the upper limit of the region where the phase agreement exists between the model and data concentrations. This value can be recommended as the upper boundary of the contact load layer for the purpose of net sediment transport calculations.

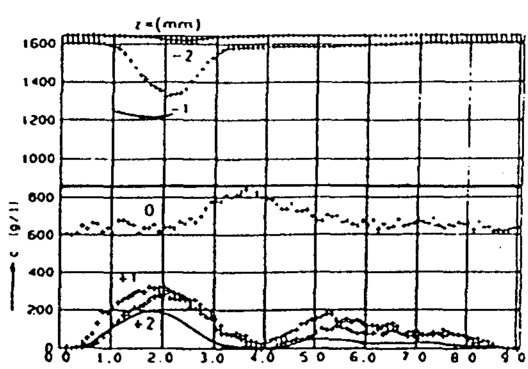

Fig. 8. Time-dependent concentrations: model results for z=-1, 0, +1 mm (solid lines) vs. measurements of Condition 2 (symbols), experimental data after Al-Salem (1993)

The model also provides reasonably accurate vertical profile of time-averaged concentration <c> up to the level of $\delta_1/2$, as shown in Fig. 9 for Condition 2 of Al-Salem's (1993) laboratory experiments.

Further evidence of good model predictions in the context of time-averaged concentration is depicted in Fig. 10 where the model results for z=1 cm are compared with experimental data of 10 wave series B and 3 series C of measurements of Ribberink & Al-Salem (1994, 1995).

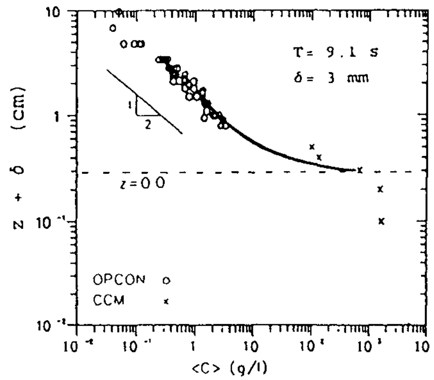

Fig. 9. Time-averaged concentration profiles: model results (solid line) vs. measurements of Condition 2 (symbols), experimental data after Al-Salem (1993)

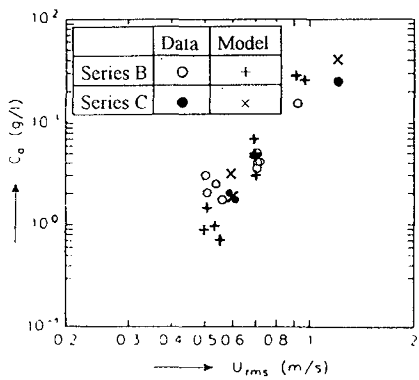

Fig. 10. Time-averaged concentrations at z=1 cm: model results ("+" and "x" for series B and C, respectively) vs. measurements ("o" and "•" for series B and C, respectively) of Ribberink & Al-Salem (1994, 1995)

Half-period averaged and net sediment transport

The same sets of computational parameters as used for determination of the sheet flow layer thickness has been assumed as the model input in the computations of sediment transport rate averaged over half wave period. In accordance to the discussion of the contact load layer thickness, the computations comprise the layer up to $\delta_l/2$. The model results can be presented as a function of $\theta_{2.5}$, the definition of which has been given by Nielsen (1992).

The model results are successfully compared in Fig. 11 with laboratory half-period sediment transport measurements. As one could have expected, for low shear stresses sediment transport consists mainly of bedload while for higher shear stresses it is dominated by suspended load. The contribution of suspended load is obviously bigger for fine sediments. It has been found out that this contribution at low shear stresses is a bit more pronounced for short wave period while at high shear stresses suspended load is slightly bigger for long wave period. The above results from bigger values of maximum shear stress and - on the other hand - smaller values of δ_l for short periods. The value of δ_l plays more important role in the regime of suspended load, thus bigger suspended load contribution is achieved at high $\theta_{2.5}$ for long wave periods. Since the differences between long and short wave period results are not very significant, one approximation for long and short wave period, for d=0.2 mm, is given in Fig. 11.

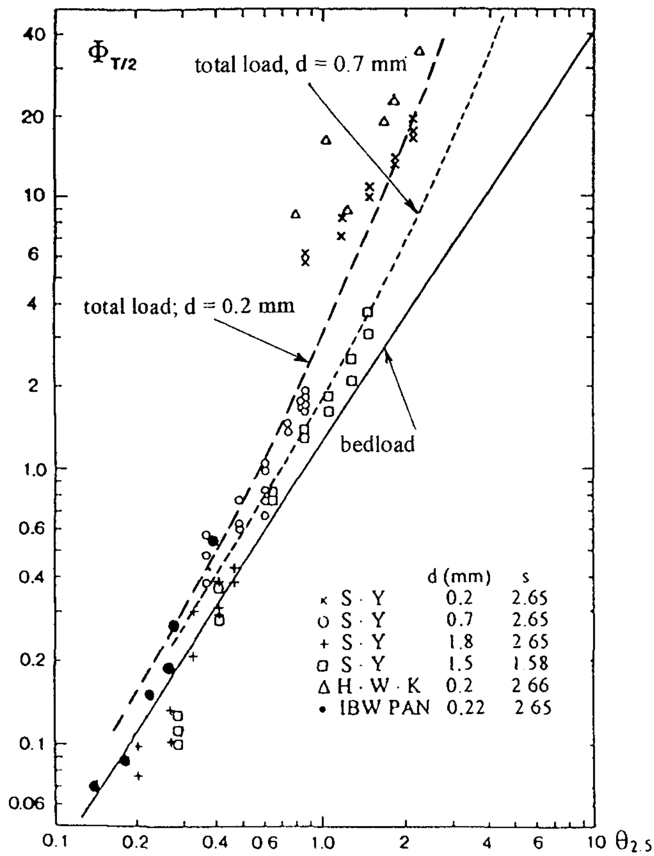

Fig. 11. Sediment transport rate averaged over half wave period model results vs. laboratory data of Sawamoto & Yamashita and Horikawa et al., definition of $\phi_{T/2}$ and experimental data as given by Nielsen (1992), and IBW PAN laboratory data

Finally, the comparison between predicted and observed net sediment transport rates for Ribberink & Al-Salem's (1994) experiments is presented in Fig. 12. Here, following the discussion on the upper validity limit for net transport determination, the computations have been carried out up to the level of z=δ_l/4 only. Except for one experiment, the compliance between calculated and measured values is good.

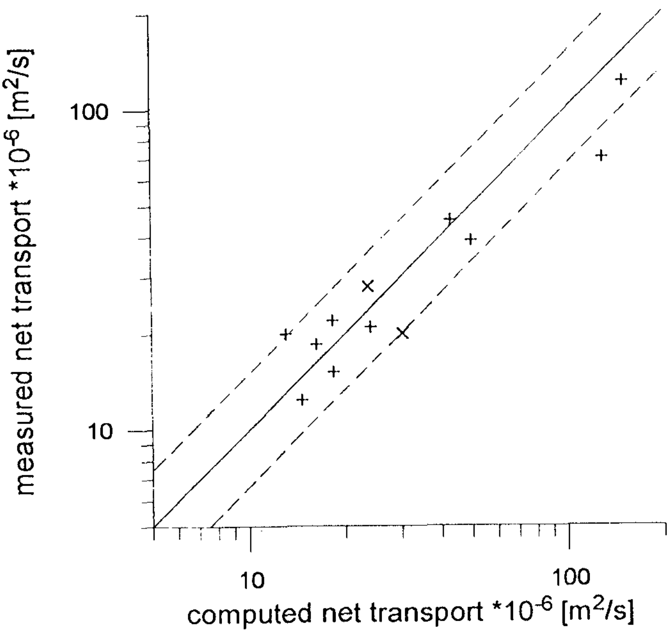

Fig. 12. Comparison between predicted and observed net sediment transport rates for 10 of Ribberink & Al-Salem's (1994) series B experiments ("+") and for 2 of the series C ("x"); the dashed lines indicate factor ±1.5

Conclusions

The contact load layer model, being an extension of the bedload model, is proposed for the calculation of sediment transport features, such as sheet flow layer thickness, sediment concentration and velocity distributions under sinusoidal and asymmetric waves. The bedload model is a basis of the proposed approach as it provides the boundary conditions for the solution of the contact load layer which makes use of the equations proposed by Deigaard (1993). The iterative procedure has been developed to determine two calibration coefficients, basically unknown in the Deigaard's (1993) proposal.

The comparisons made between the model results and available laboratory data in all analysed cases yield at least satisfactory agreement. Significant discrepancies between the model results and the experimental data, in the context of time-dependent concentrations, are found at higher levels of the contact load layer. They are most probably linked to convective events in flow reversal. Now, there is a need to carry out further studies in order to include the description of convective terms in the present model.

References

Al-Salem, A. (1993). Sediment transport in oscillatory boundary layers under sheet-flow conditions, *Ph.D. Thesis*, Delft Hydraulics.

Bagnold, R.A. (1956). The Flow of Cohesionless Grains in Fluids, *Phil. Trans. Roy. Soc.*, London, Ser. A, Vol. 249, 235-297.

Davies, A.G., J.S. Ribberink, A. Temperville & J.A. Zyserman (1997). Comparisons between sediment transport models and observations made in wave and current flows above plane beds, *Coastal Engineering* 31, 163-198.

Deigaard, R. (1993). Modelling of sheet flow: dispersion stresses vs. the diffusion concept, *Prog. Rep.* 74, Inst. Hydrodyn. and Hydraulic Eng., Tech. Univ. Denmark, 65-81.

Engelund, F. & J. Fredsøe (1976). A sediment transport model for straight alluvial channel, *Nordic Hydrology*, Vol. 7.

Fredsøe, J. (1984). Turbulent boundary layer in combined wave-current motion, *J. Hydraulic Eng.*, ASCE, Vol. 110, No. HY8, 1103-1120.

Fredsøe, J. & R. Deigaard (1992). Mechanics of coastal sediment transport, *Advanced Series on Ocean* Engineering, Vol. 3, World Scientific, Singapore..

Kaczmarek, L.M., J.M. Harris & B.A. O'Connor (1994). Modelling Moveable Bed Roughness and Friction for Spectral Waves, *Proceedings of 24th International Conference on Coastal Engineering*, ASCE, 300-314.

Kaczmarek, L.M., R. Ostrowski & R.B. Zeidler (1995). Boundary Layer Theory and Field Bedload, *Proc. International Conference on Coastal Research in Terms of Large Scale Experiments (Coastal Dynamics '95)*, ASCE, 664-675.

Kaczmarek, L.M. & R. Ostrowski (1996). Asymmetric and Irregular Wave Effects on Bedload: Theory versus Laboratory and Field Experiments, *Proc. 25th ICCE*, ASCE, 3467-3480.

Nielsen, P. (1992). Coastal bottom boundary layers and sediment transport. *Advanced Series on Ocean* Engineering, Vol. 4, World Scientific, Singapore.

Ribberink, J.S. & A. Al-Salem (1994). Sediment transport in oscillatory boundary layers in cases of rippled beds and sheet flow, *Journal Geoph. Res.*, Vol. 99, No. C6, 12,707-12,727.

Ribberink, J.S. & A. Al-Salem (1995). Sheet flow and suspension of sand in oscillatory boundary layers, *Coastal Engineering*, No. 25, 205-225.

Sumer, B.M., A. Kozakiewicz, J. Fredsøe & R. Deigaard (1996). Velocity and concentration profiles in sheet-flow layer of movable bed, *J. Hydraulic Eng.*, Vol. 122, No. 10.

Wilson, K.C. (1987). Analysis of Bed-Load Motion at High Shear Stress, *J. Hydraulic Eng.*, Vol. 113, No. 1, 97-103

Zyserman, J.A. & J. Fredsøe (1994). Data analysis of bed concentration of suspended sediment, *J. Hydraul. Res.*, Vol. 120, No. 9, 1021-1042.

Acknowledgements

This study contributes to the research project *INDIA* carried out under the EU Environment and Marine Science and Technology (MAST III) programme and is sponsored by KBN, Poland, under SPUB and programme 2 *IBW PAN*.